

Article

Radioactive Isotopes as a Tool for Pairing Identification of the HAH 346—Hammadah al Hamra 346—Ordinary Chondrites from Two Separate Find Areas

Magdalena Długosz-Lisiecka ^{1,*}, Tomasz Jakubowski ², Marcin Krystek ³ and Ahmed ElMallul ^{4,5}

¹ Faculty of Chemistry, Institute of Applied Radiation Chemistry, Lodz University of Technology, Wroblewskiego 15, 90-924 Lodz, Poland

² Independent Researcher, Lukowska 22, 54-102 Wrocław, Poland

³ Geological Museum, Faculty of Geographical Sciences, University of Łódź, Kopcińskiego 31, 90-142 Łódź, Poland

⁴ Faculty of Medical Technology, Al Zentan University, Al Zentan, Libya

⁵ Libyan Society for Meteorites & Space Observation, Al Zentan, Libya

* Correspondence: magdalena.dlugosz@p.lodz.pl

Abstract: In this study, low-background gamma spectrometry was used to confirm the identity of a set of ordinary chondrites found in 2018 and 2019, by different expeditions, in a part of the Al-Hamada al-Hamra desert, in the region of Al-Dżabal al-Gharbi, in Libya. Ten specimens of ordinary chondrites from two different campaigns were investigated. An analysis was carried out using a unique gamma spectrometry system to obtain the optimal measurement conditions for the quantitative identification of the radioactive isotopes. Chondrite radiometric studies enabled a detailed analysis of the activities of radioactive isotopes—the short-lived ^{22}Na , ^{54}Mn , ^{60}Co , and long-lived ^{26}Al , ^{40}K . For most isotopes, the activities are expected to be similar for ordinary chondrites with the same irradiation history. Short-lived radionuclide concentrations can be considered, as a specific fingerprint of the chondrite terrestrial age, to confirm whether meteorites originate from a single fall. The HaH 346 group of chondrites was classified in February 2021. The data sets have been analyzed based on multivariate chemometric techniques, including K-means, PCA, and clustering analysis, to derive essential information and confirm similarities or significant differences between the studied specimens.

Keywords: low-background gamma spectrometry; ordinary chondrites; radionuclide; radioactive isotopes; chemometric analysis; HaH 346



Citation: Długosz-Lisiecka, M.; Jakubowski, T.; Krystek, M.; ElMallul, A. Radioactive Isotopes as a Tool for Pairing Identification of the HAH 346—Hammadah al Hamra 346—Ordinary Chondrites from Two Separate Find Areas. *Minerals* **2022**, *12*, 1553. <https://doi.org/10.3390/min12121553>

Academic Editor: Jesus Martinez-Frias

Received: 31 October 2022

Accepted: 28 November 2022

Published: 1 December 2022

Publisher's Note: MDPI stays neutral with regard to jurisdictional claims in published maps and institutional affiliations.



Copyright: © 2022 by the authors. Licensee MDPI, Basel, Switzerland. This article is an open access article distributed under the terms and conditions of the Creative Commons Attribution (CC BY) license (<https://creativecommons.org/licenses/by/4.0/>).

1. Introduction

According to the Meteoritical Bulletin Database, a large number of meteorites are collected in the Sahara Desert, especially in the part of Al-Hamada al-Hamra in Libya (HaH). Up until now, 1559 meteorites have been found in the Libya desert, and 13,435 NWA meteorites have been officially recorded in the Meteoritical Bulletin Database (on November 2022), making this area one of the best places in the world for finding meteorites. Small numbers of observed falls such as Werdana and the HaH 346 were also noted in other deserts such as Oman. The found locations for many of the meteorites in the Sahara are unknown, while for most of the meteorites from DaG and HaH, the found locations are recorded, which makes it easier to identify large pairing groups [1].

There were reports of two different falls in the region among the local population: in November 2017 and in August 2018. Thus, two observed falls of large ordinary chondrites occurred in the Hammadah al Hamra area in quite a short time. Most importantly, a comparison of macroscopic observations such as fusion crust, texture, and impact pits on the fusion crust showed that the material from both falls was relatively similar. Therefore, after

classification studies, additional efforts were made to analyze the radioactive isotopes in a large number of specimens collected during the different excursions in order to categorize the sets of chondrites. This was performed using an independent and nondestructive low-background gamma-ray spectrometry system with a unique passive shield.

Chondrites in Libya are found in several areas, such as Dar al Gani and Hammadah al Hamra (Dense Collection Areas—DCA) [2]. The Libyan Society for Meteorites and Space Observation systematically searches for meteorites in the desert. In 2019, a set of chondrites was found close to a town called Ashuwairif (location: N 29°33'678"; E 013°28'515"). The fall was estimated to have occurred on 26 August 2018. In February 2021, the chondrites from that unconfirmed fall were classified as HaH 346 (Meteoritical Bulletin no. 110). In 2019, an expedition close to Gheriat town resulted in a collection of additional specimens. The distance between both locations of the falls close to Ashuwairif and Gheriat was estimated at 50 km.

Ordinary chondrites come from parent bodies in the asteroid belt located between Mars and Jupiter [3]. The meteoroids are irradiated by GCRs during their travel in space after their ejection from the parent body. GCR generates spallation reactions on target elements, which produce cosmogenic noble gases and radionuclides. Meteoroids contain cosmogenic and primordial radionuclides due to various processes that have occurred throughout their history [4,5]. Cosmic rays composed of solar and galactic cosmic rays generate spallation reactions on meteoroid target elements, such as aluminum, silicon, calcium, and heavy-target elements [6,7]. As a result, radioactive isotopes are produced, such as ^{22}Na , ^{54}Mn , and ^{60}Co [8–13].

Various short-lived radionuclides can be generated in parent or meteor bodies, e.g., ^{22}Na , ^{54}Mn , and ^{60}Co . This process stops as soon as the meteorite reaches the Earth. Since then, the activities have decreased at a rate of their own half-life. In freshly fallen specimens (found just after falling), the activities of the radionuclides depend on the energy and the composition of cosmic particles of solar and galactic origins.

The ^{22}Na isotope is produced from several elements, including Mg, Si, S, and Fe, Ni. ^{22}Na is sensitive to cosmic ray variations over the 11-year Schwabe cycle [14]. ^{54}Mn has been produced from Cr, Fe, Co, Ni, Cu, or even Zn and other elements present in the parent body structure in various nuclear reactions [15,16].

The contribution of the Co element in ordinary chondrites varies from 0.08 to 0.11 %. The Co isotope contributes to almost all of the Co budget. Cosmogenic ^{60}Co is mainly produced by thermal neutron capture in the reaction $^{59}\text{Co}(\text{n},\gamma)^{60}\text{Co}$, and to a lesser extent in $^{60}\text{Ni}(\text{n},\text{p})^{60}\text{Co}$ or in the spallation process $^{62}\text{Ni}(\text{n},\text{p}2\text{n})^{60}\text{Co}$ [17]. According to Dilg et al. [17], for large meteoroids, the dominant reaction is neutron uptake, and the minimal size for a material with a composition corresponding to stony meteorites is a 25 cm diameter object. The concentration of ^{60}Co in all types of meteorites depends on the date of the meteorite fall, as the 11-year cycle of solar activity has an effect on it. The relatively short half-life of ^{60}Co is 5.27 years (similar to ^{22}Na), and this influences the dynamics of ^{60}Co production [18–20]. Neutrons with an energy lower than 10^{-5} MeV are more effectively captured by ^{59}Co ; thus, the ^{60}Co activity concentration increases dramatically with the diameter of the meteorite body, which has a moderate structure of the neutrons. Therefore, the activity of the cosmogenic ^{60}Co isotope should increase logarithmically. On the other hand, ^{60}Co activities can change with the density, chemical composition, and diameter of the meteoroid.

The concentration of radioactive isotopes or isotope ratios in a chondrite is commonly used to identify specimens from the same fall [21]. The various spectrometric methods used in isotopic studies of meteorites provide information, such as the nature of the parent body, the length of time spent in space, the nature of the meteoroid's orbit in relation to the Sun, and the terrestrial age. Low-background gamma spectrometric techniques allow meteorites to be compared and classified in different ways than in classic petrographic, mineralogical, and geochemical analyses [21–28].

The advantage of radiometric analysis is that it can determine particular aspects of meteoritic minerals, especially the duration of exposure to cosmic radiation (cosmic-ray exposure age) and the elapsed time since the end of exposure (terrestrial age). Low-background gamma spectrometry allows for the nondestructive analysis of collectible specimens. Improvement in the precision of a radiometric analysis allows smaller isotopic differences between meteorites to be distinguished [18–20,29].

The aim of this study was to confirm that the specimens collected during the two different campaigns in the HAH 346 chondrites: for such study, we used chemometric methods based on short-lived ^{22}Na , ^{54}Mn , and ^{60}Co radionuclides. Preliminary classification of chondrites made with the approval from the Committee of Nomenclature showed that all specimens found had similar petrographic and mineralogical features and represented ordinary chondrite type L5 and shock stage S1–S4 or even S5. The chondrites were assigned the W0 weathering scale, but this differed slightly for individual specimens (due to the different times of collecting the chondrites from the desert) [30–32].

2. Material and Methods

2.1. Samples

A set of ten chondrite specimens (Table 1) were investigated: three specimens from a location close to Gheriat (HAH 346-3, HAH 346-6, HAH 346-7) were collected by the person from the Libyan Society for Meteorites and Space Observation and seven specimens from a location close to Ashuwairif (HaH 346-134, HaH 346-201, HaH 346-200, HaH 346-207, HaH 346-120, HaH 346-163 and HaH 346-198; Figure 1) were collected by private meteorite hunters. The locations of the specimens were 50 km away from each other.

Table 1. List of the samples.

Laboratory Code of the Specimen	Sample Mass [g]		Date of the Sample Collection from the Desert
	Bulk Sample	Powder	
HaH 346-3	23	50	2018
HaH 346-6	141	-	2018
HaH 346-7	221	-	2018
HaH 346-134	134	-	2019
HaH 346-198	198	-	2019
HaH 346-201	201	-	2019
HaH 346-200	200	-	2019
HaH 346-207	207	-	2019
HaH 346-163	163	-	2019
HaH 346-120	120	-	2019

Macroscopic photographs (Figure 2) of chondrites from two expeditions from the area of Al-Dżabal al-Gharbi, Libya. Left—one of the analyzed pieces of HaH 346 (found close to the Ashuwairif town). Dimensions = 59 mm × 38 mm × 35 mm. A dark melting crust with a slightly rough texture and a delicately marked network of polygonal fractures surrounds the light gray interior of the chondrite with single small, rusty brown spots formed as a result of weathering. Right—one of the examined pieces (found close to Gheriat town and a short distance from the main site). Dimensions = 60 mm × 47 mm × 38 mm. The surface is regmaglypts, and debris is formed as a result of the selectivity of the smelting process. The melting crust, visible on the surface and cut with a distinct network of contraction cracks, hides the light-gray interior of the chondrites with small rusty-colored spots and shock veins.

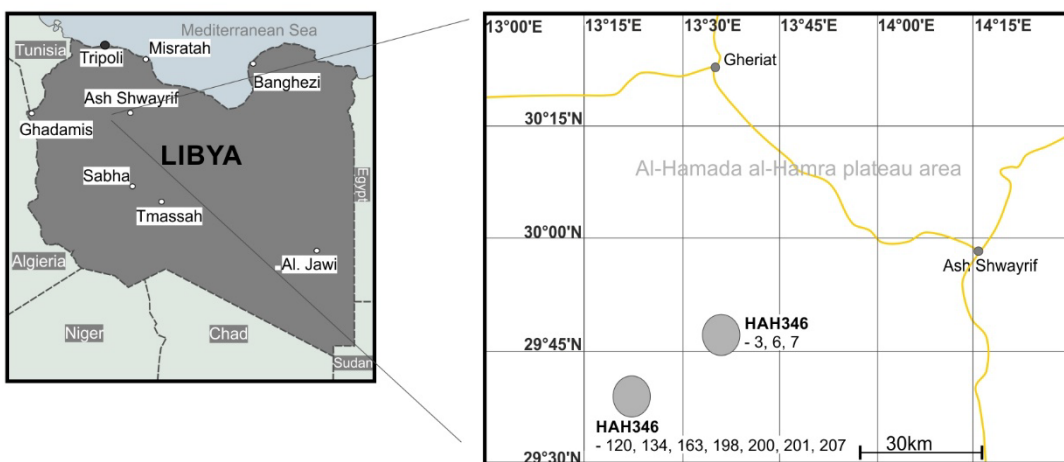


Figure 1. Map of the HaH 346 items found.



Figure 2. Photo of two HaH 346 specimens from two different expeditions (a) Close to Ashuwaifir town (HaH 346-201), (b) Close to Gheriat town (HaH 346-3).

2.2. Method of Analysis

All spectrometric measurements were carried out in the Laboratory of Radiometric Methods at the Institute of Applied Radiation Chemistry at the Lodz University of Technology between 2019 and 2020 [33–35]. Since 2017, the radiometric laboratory has introduced a quality management system for radiometric measurements in accordance with the ISO 17025 standard.

In this study, the activities of the radionuclides ^{22}Na , ^{54}Mn , and ^{60}Co were measured using a unique low-background spectrometry system consisting of a high-purity germanium (HPGe) detector (30% relative efficiency; CANBERRA Industries; Figure 2). The system operating in anticoincidence with a guarded 9-inch NaI(Tl) scintillator (non-standard model, produced on a special order in SCIONIX, Figure 2) in order to achieve the active reduction of Compton scattering, the reduction of minimum detectable activity (MDA) parameter and relatively low uncertainty of results [14,36–40]. A list of the isotopes and their gamma energy lines analyzed in this study are shown in Table 2.

All measurements were carried out on entire specimens, and the applied method was noninvasive. However, some meteorites (with the owner's agreement) were cut and ground for better geometry and results. In this case, the detection efficiency for the whole specimens was determined by the LabSOCS method [41,42], compared with those obtained using the standard reference materials at the same geometry [33–35].

Table 2. Analyzed isotopes along with their gamma energy lines, half-lives (NDS base (IAEA Nuclear Data Services)) and an example of MDA results.

Isotope	Gamma Energy Peaks (keV)	Yield of Gamma Emission (%)	T _{1/2}	MDA [dpm/kg]
²² Na	1274	99.94	2.602 years	1.11
²⁶ Al	1808	99.76	7.17·10 ⁵ years	1.44
⁴⁰ K	1460	10.66	1.25·10 ⁹ years	11.54
⁵⁴ Mn	834	99.97	312.2 days	0.43
⁶⁰ Co	1173	99.85	5.30 years	1.04
	1332	99.98		1.15

The unique, low-background spectrometric system (Figure 3) used in this study provided the opportunity to work in three independent modes—coincidence, anticoincidence, and singles. Conducting measurements in various modes led to optimal measurement conditions for the quantitative and qualitative identification of radioactive isotopes (Table 2), mostly anticoincidence. Detection efficiency calibration is used for quantitative analysis of the chondrites. In practice, the gamma spectrometry system allows for the quality and quantity analysis of the spectrums. Routinely, the background has been subtracted from the raw spectra. Each measurement for an individual sample was carried out over at least four days, over 320,000 s to a maximum of 800,000 s; thus, the uncertainty of the measurement did not exceed 5% for ⁴⁰K, 10% for ²²Na, ²⁶Al, and ⁵⁴Mn.



Figure 3. Unique gamma spectrometry system with an active anticoincidence shield.

2.3. Quality Assurance

For the gamma spectrometry analysis, the chondrite samples were measured in two geometry versions: the original, as a stone version, and the second, in a powder version (with permission from the owner). For the powder version, the material was cut off from a larger fragment using a precision automatic saw with a diamond blade. The material was then ground to powder using a ball mill (RETSCH) for 20 min. In the cutting and grinding process, the highest care for the material purity was achieved. A portion of approximately 50 g of powder was used for the radiometric analysis. The remaining portion was preserved for exhibition purposes. Samples were analyzed in a cylindrical geometry, with a diameter size of 60 mm and a height of about 30 mm, depending on the available portion [33–35]. The mass of the chondrite samples varied from 44.1 g to 221 g in the ten HaH 346 specimens.

Due to the lack of a suitable standard available for the direct calibration of the gamma spectrometry system, several measures were undertaken to improve the quality and precision of the measurements. The use of the powder material and cylindrical geometry was validated in intercomparison tests (e.g., IAEA TEL 2017 PT). For detection efficiency, two different approaches were applied: simulation based on the LabSOCS method or experimentally based on the standard reference materials [33–35].

In the experimental approach, detection efficiency was verified for various natural and artificial radionuclides. The powder form of the material and measurements performed on the samples with cylindrical geometry allowed the system to be efficiently calibrated based on the International Atomic Energy Agency, IAEA, certified reference materials or materials from intercomparison tests. The precision of the experimental method was proven in the direct experiment using Ca-carbonate powder (IAEA TEL 2017-03 PT) measured at the same geometry as the powder of the chondrite specimens. The Ca-carbonate powder contains ^{226}Ra at an activity concentration of 6970 Bq/kg, as well as other natural radionuclides [33–35]. After four weeks, the short-lived daughter isotopes ^{214}Bi (1765 keV peak energy line) (experimental value 7033 ± 325 Bq/kg) and ^{214}Pb (experimental value 6752 ± 451 Bq/kg) occurred in secular equilibrium with ^{226}Ra , and this was used to obtain the detection efficiency curve.

Due to the various geometries of the samples, the detection efficiency of the specimens was established on the basis of LabSOCS (Laboratory Sourceless Calibration Software) (CANBERRA Industries, Inc., Meriden, CT, USA). This method allowed the detection efficiency values (Figure 4) to be corrected based on the different chemical composition of the analyzed materials [33–35]. The chemical compositions of the meteorites were analyzed using the X-ray fluorescence XRF technique.

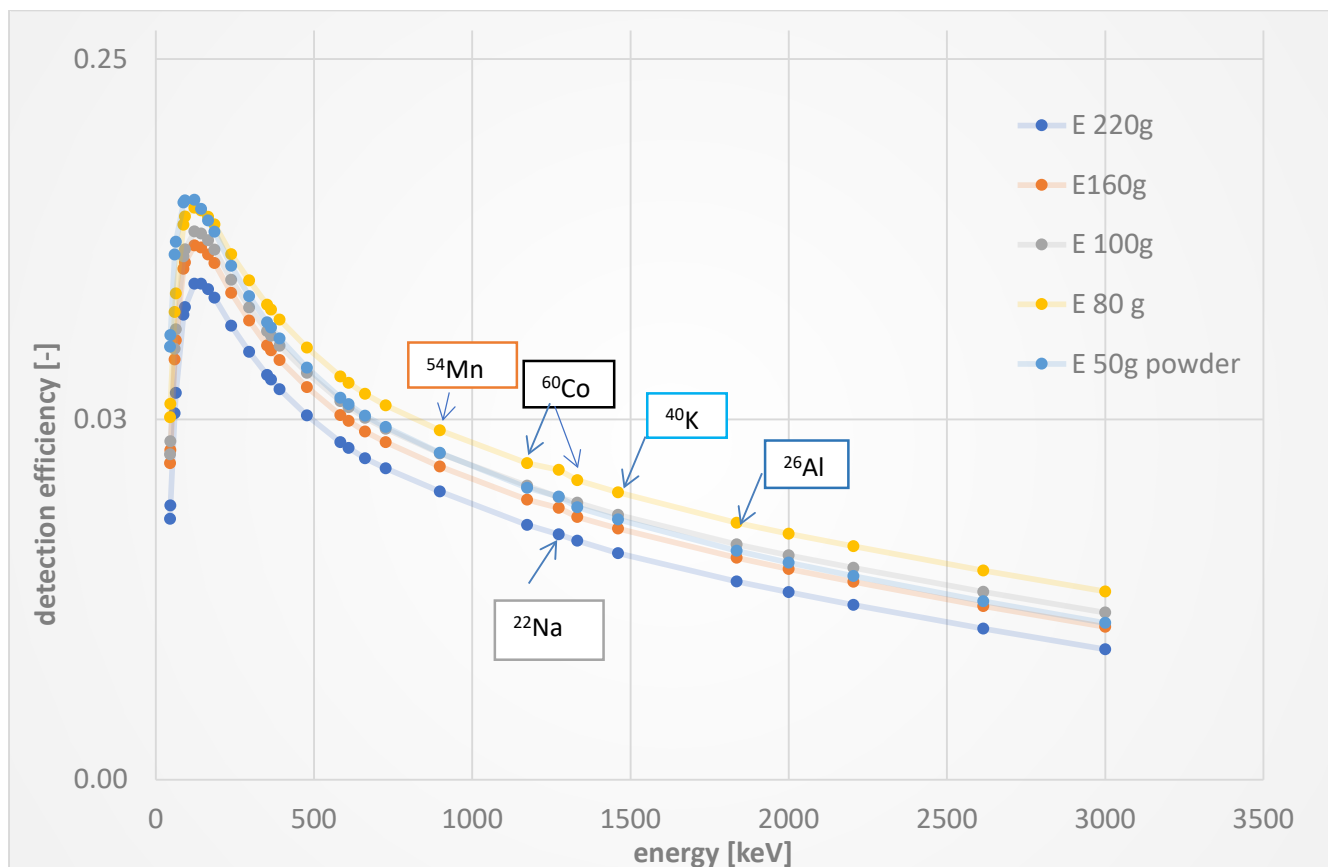


Figure 4. Detection efficiency curves for various meteorite geometries using LABSOCS (CANBERRA) software.

2.4. Chemometric Approach

The PCA method has been applied to provide a representation of the chosen variables: ^{22}Na , ^{26}Al , ^{40}K , ^{54}Mn , and ^{60}Co , which allows variables to be found that are characteristic of chondrites groups [21,43]. K-means clustering is a method of assigning each observation-isotopes concentration to the cluster with the nearest mean. Algorithm K-means clustering tends to find clusters of comparable spatial extent. In this approach, the Euclidean distance is used as a metric, and the variance is used as a measure of the cluster scatter. Therefore, K-means can be used to choose k different centers from a large data set for further interpretation.

Cluster analysis is a hierarchical analysis grouping of the objects, which are the results of the analysis, belonging most likely to the same distribution. The graphical representation of the method allows groups to be established with small distances between the clusters, which is useful for the interpretation of similarities or the confirmation of significant differences.

3. Results

The chemometric analysis of a low amount of specimens is highly demanding due to the natural inhomogeneity in the parent body structure, resulting from various processes occurring inside during its history. Mn, Al, K, Na, and Co, differ from their chemical and physical properties, including boiling point, evaporation temperature, and chemical form. Several processes effectively occur on the surface of the parent body (evaporation, isotopic activation), and others are influenced by the diameter where the parent body structure performs the role of a massive shield (neutron moderation and neutron capture by ^{59}Co). Some parent bodies can show natural primordial inhomogeneity in isotopic compositions, confirmed by several studies. Several works [5–15,44] confirm that some chondrites could represent the outer, unmelted crusts and differentiated planetesimals with silicate mantles and metallic cores.

Radioactive isotope concentrations and ratios are unique for various meteorites, including ordinary chondrites. The radiometric analysis of ordinary chondrites can help to confirm whether two samples originate from the same parent body or a different fall. However, natural variability in isotopic specific activity connected with the primordial differentiation of the parent body structure is possible. In this study, the activity of selected isotopes: short-lived ^{22}Na , ^{26}Al , ^{40}K , ^{54}Mn , and ^{60}Co , was measured and used to characterize the investigated samples. Several statistical tools can help in a clear interpretation of variability for the obtained analytical results. All results have been corrected and normalized to the same day: 14 November 2017 (the day of the first observed fall).

The concentration of short-lived isotopes ^{22}Na , ^{54}Mn , and ^{60}Co in the chondrites varied from 37.1 ± 3.5 to 59.3 ± 5.1 dpm/kg, 13.3 ± 0.9 to 44.4 ± 4.4 dpm/kg, and 7.1 ± 0.5 to 156 ± 10 dpm/kg, respectively (Table 3.). Concentrations of longer-lived radionuclides ^{26}Al and ^{40}K range from 35.6 ± 3.2 to 63.1 ± 6.1 dpm/kg and from 1336 ± 66 to 1799 ± 89 dpm/kg, respectively (Table 3).

The ^{60}Co radionuclide is especially useful for interpreting exposure history, pre-atmospheric sizes of the meteorites, and sampled shielding depths [44]. A high content of ^{60}Co (average 58.1 dpm/kg) may indicate a large meteorite diameter exceeding 1 m.

Both isotopes, ^{22}Na , and ^{54}Mn act as an isotopic signature for the confirmation of the joint (or different) fall of all specimens. ^{22}Na , ^{54}Mn with the shortest half-lives (Table 2) are important tracers for the terrestrial age of the investigated specimens. Figure 5 shows a correlation between ^{54}Mn and ^{22}Na activities and exhibits two different groups. The relatively lower ^{22}Na and ^{54}Mn activity concentration in HaH 346-163 and HaH 346-198 indicates an older terrestrial age or a lower initial content of these isotopes in the chondrites. Variations in ^{22}Na , ^{54}Mn , and ^{60}Co in the ten HaH 346 meteorite fragments are due to variations in the shielding depth in a meter-sized object.

Table 3. Short-lived radionuclides ^{22}Na , ^{54}Mn , ^{60}Co and long-lived radionuclides ^{40}K , and ^{26}Al activity in various HaH 346 specimens.

Id	^{22}Na	Activity Concentration of Radionuclides [Bq/kg]			
		^{26}Al	^{54}Mn	^{40}K	^{60}Co
HaH 346-3	59.3 ± 5.1	44.3 ± 4.1	44.4 ± 4.4	1440 ± 71	156 ± 10
HaH 346-6	50.9 ± 4.9	46.6 ± 4.3	43.4 ± 3.9	1532 ± 70	17.2 ± 1.5
HaH 346-7	50.3 ± 4.4	43.6 ± 4.2	43.0 ± 3.8	1475 ± 72	70.6 ± 6
HaH 346-134	59.6 ± 5.3	45.1 ± 4.4	36.8 ± 3.3	1336 ± 66	85.4 ± 7.9
HaH 346-198	37.1 ± 3.5	63.1 ± 6.1	22.5 ± 2.0	1630 ± 80	7.1 ± 0.5
HaH 346-201	53.2 ± 5.1	39.6 ± 3.1	26.7 ± 2.1	1584 ± 75	28.4 ± 2.1
HaH 346-200	48.7 ± 4.3	39.3 ± 3.3	27.5 ± 2.5	1420 ± 70	52.0 ± 5.1
HaH 346-207	58.1 ± 5.6	48.0 ± 4.5	31.9 ± 2.9	1477 ± 73	13.4 ± 0.9
HaH 346-163	37.8 ± 3.5	41.0 ± 3.8	13.3 ± 0.9	1799 ± 89	15.0 ± 1.2
HaH 346-120	49.1 ± 4.6	35.6 ± 3.2	33.3 ± 2.9	1517 ± 70	43.5 ± 4.2

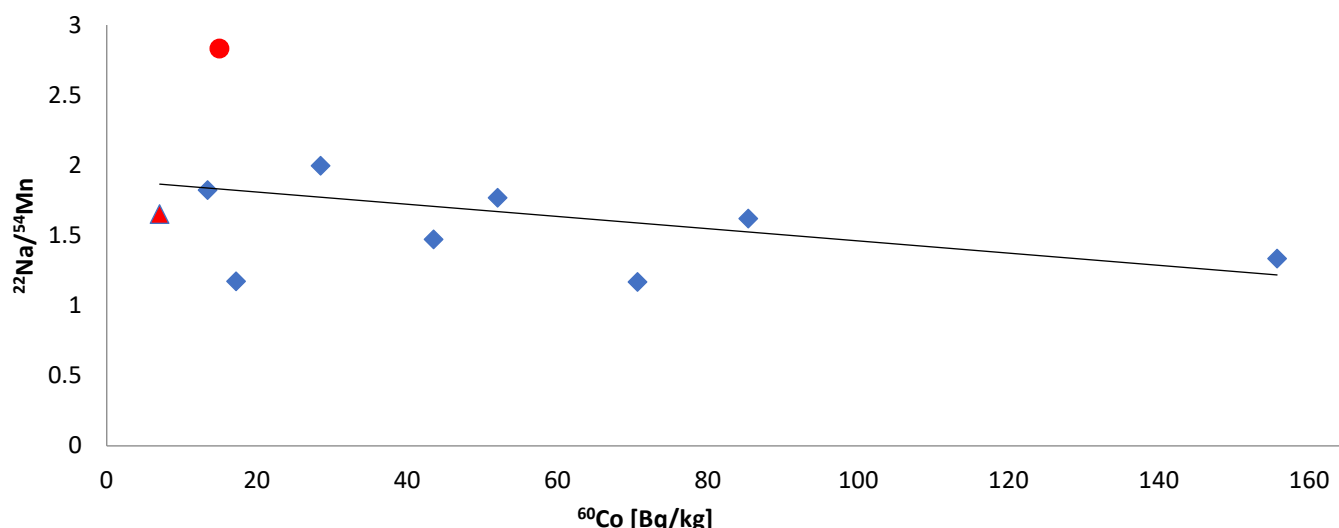


Figure 5. ^{54}Mn and ^{22}Na activity ratio in function of ^{60}Co as indicators of terrestrial age of chondrites [dpm/kg], red circle—HaH 346-163 and red triangle—HaH 346-198, blue rhombus—other samples.

The variation in ^{60}Co activity (from ~7 to ~156 dpm/kg) can be explained by variations in the shielding depth within a meter-sized object; therefore, samples with code HaH 346-198 and HaH 346-163 represent fragments from shallow depths. These depth variations also affect the production of ^{22}Na and ^{54}Mn isotope concentrations.

$^{22}\text{Na}/^{26}\text{Al}$ activity ratios for both specimens are lower than one and are equal to 0.92 and 0.60, respectively, while for the other eight samples of chondrites, the values ranged from 1.09 to 1.37. This fact can be the result of chemical differences between both elements (the higher volatility of vapor in Na elements in comparison to the Al element).

To explain the lower ^{22}Na and ^{54}Mn isotope concentrations, a statistical *t*-test has been applied for the confirmation of significant differences between both groups of results. Significant differences for both isotopes and both groups have been confirmed with the probability $p < 0.05$ for ^{22}Na and ^{54}Mn , $p < 0.008$ and $p < 0.006$, respectively, and for both isotopes independently in Figure 6. In each case, eight results representing one group were compared with two results from the second group, represented by only HaH 346-163 and HaH 346-198 (Figure 5).

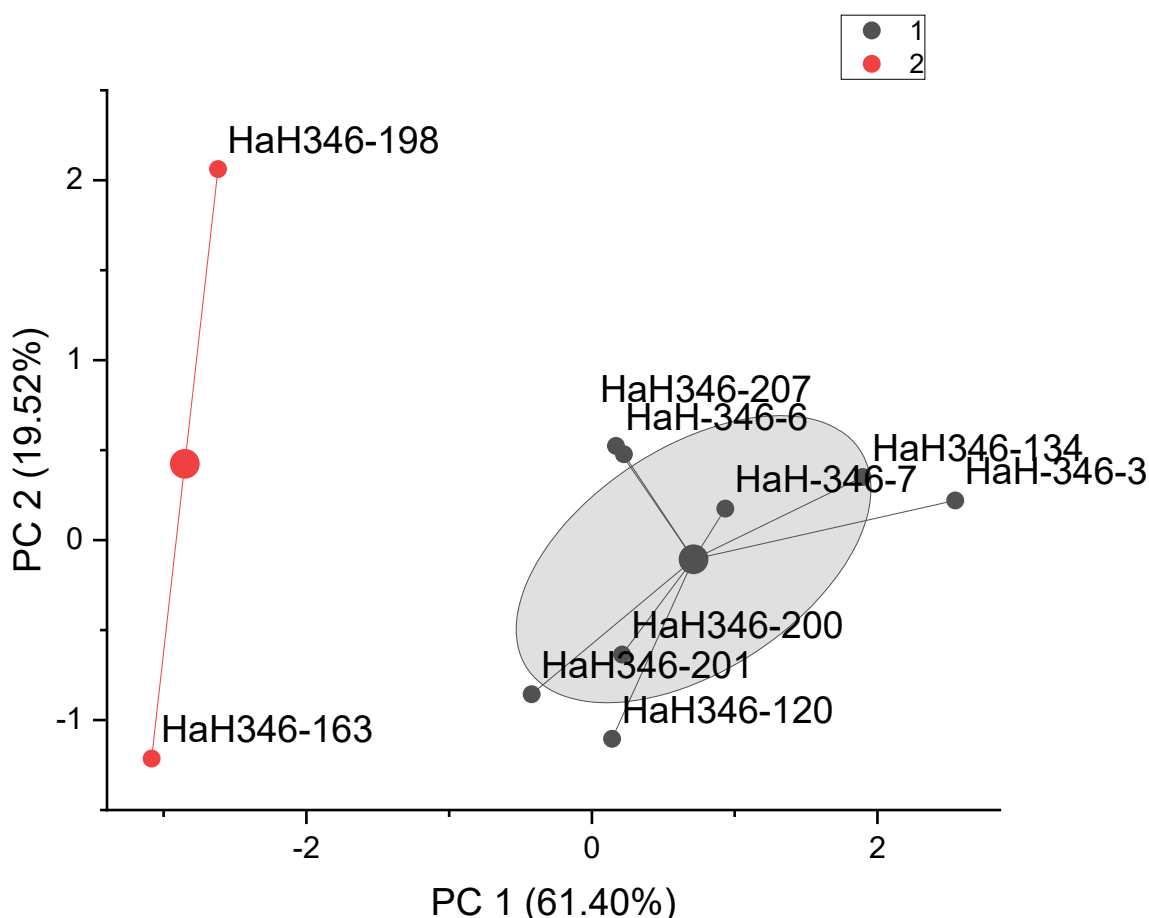


Figure 6. K-means cluster plot: PC2 (19.52%) in function of PC1 (61.40%).

In the next step, ^{22}Na , ^{26}Al , ^{40}K , ^{54}Mn , and ^{60}Co isotope concentrations were applied as input variables for a chemometric analysis: K-means, PCA, and cluster analysis method.

The K-means method is a useful technique for elucidating subtle but pertinent information that is present in analytical results and groups similar data points together. The final clustering scores of the set data were derived from the first PC (PC-1, 61.40%) and the second PC (PC-2, 19.52%) and are illustrated in Figure 7.

In the case of the K-means method, the k-numbering of centroids (the center of the clusters) is established. The algorithm locates the data point to the nearest cluster, keeping the centroids as small as possible and optimizing the positions of the centroids. Similar principal components were identified by the principal component analysis, where two principal components, PC1 (61.40%) and PC2 (19.52%) (Figure 6), described over 80% of the variance. Organizing information using the PCA analysis allows the same information in the form of new PC variables to be shown, which can help in the interpretation of the variability factors in the input data structure. The larger the variance carried by the PCA analysis, the more information it allegedly has [35].

The PCA analysis distributes the radionuclide concentrations in a new variable structure, which is useful for the interpretation of the differences between the specimens (Figure 7). Extracted from the PCA analysis, eigenvectors show a correlation between the old and the new variables. The results suggest a similar relation between all three isotopes and the PC1 coefficient with factors close to 0.6. In the case of PC2, a significant correlation has been linked with ^{60}Co . The principal component PC1 can be interpreted as a factor of the terrestrial age of the chondrites, where higher isotope concentrations correspond with a shorter terrestrial age (Table 4). The second component, PC2, is correlated with ^{60}Co and can yield information about the depth in diameter of the parent

body structure. The ^{60}Co isotope in meteorite studies is usually used as a factor of the pre-atmospheric size. Higher ^{60}Co concentration in the HaH 346-3 specimen can be explained by the location of the sample at the center of the meteoroid, where ^{60}Co production from the thermal neutron capture process occurs in a high-density structure.

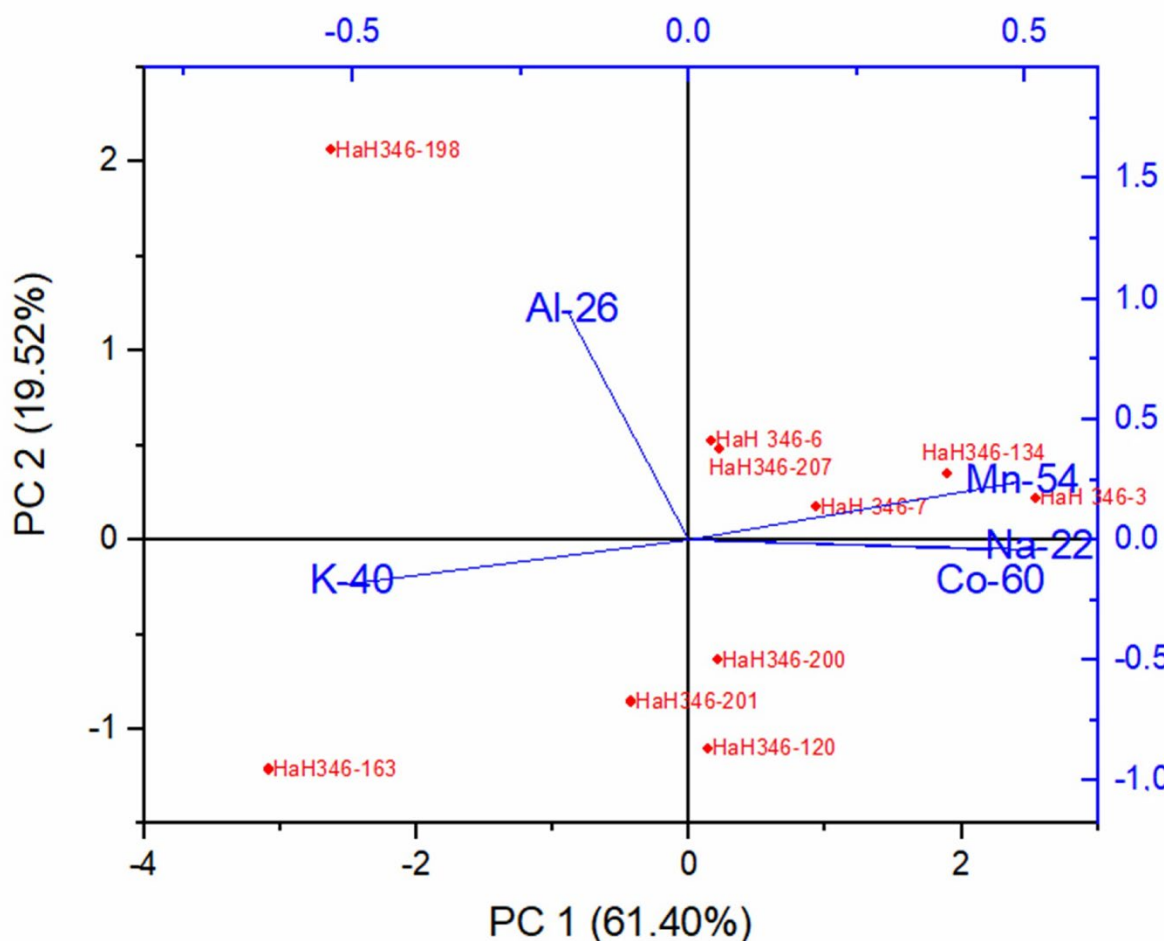


Figure 7. PCA analysis results.

Table 4. Extracted eigenvectors.

	Coefficient of PC1	Coefficient of PC2
^{54}Mn	0.490	0.241
^{22}Na	0.516	-0.038
^{60}Co	0.451	-0.042
^{40}K	-0.507	-0.181
^{26}Al	-0.179	0.952

Clustering based on the Euclidean distance aggregates data points together because of certain similarities. In the next step, the Ward method of the clustering analysis was applied in the form of a dendrogram structure.

The Euclidean distance method of the clustering analysis confirmed the grouping of the samples into two different clusters. Moreover, the multivariate dataset partitioned the large data set into meaningful subgroups. Both methods, k-means and clustering analysis, grouped eight specimens of chondrites to one centroid. HAH 346-163 and HAH 346-198 represent significantly different centroids.

After identifying the differences in the concentrations of the radioactive isotopes of short-lived radionuclides, further classification tests were carried out. The preliminary results based on the Ward clustering method indicated differences that could be due to some fragments originating from different parent bodies. The cluster analysis (Figure 8) based on the ^{22}Na , ^{26}Al , ^{40}K , ^{54}Mn , and ^{60}Co radionuclides group studied chondrites on two associated centers. The method organized results taking into consideration the Euclidean distance, which can be applied as a similarity factor between the items. All analyzed chondrites were separated into two clusters, joining more similar specimens in the centers. However, the cluster analysis excluded HaH 346-198 and HaH 346-163 from the main group; therefore, both specimens were confirmed to come from significantly different falls.

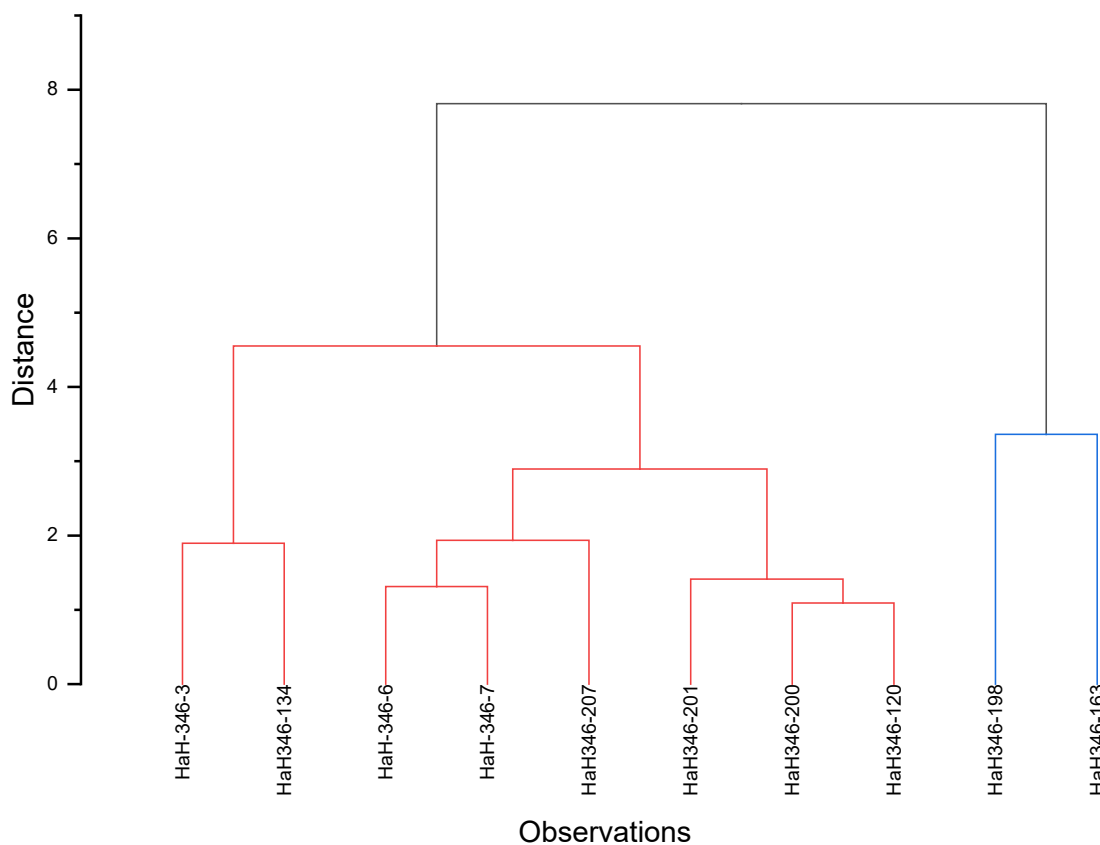


Figure 8. Cluster analysis results based on ^{22}Na , ^{26}Al , ^{40}K , ^{54}Mn , and ^{60}Co isotopes.

4. Conclusions

Hamadah al Hamra desert is a dense collection area where, each year, several possible falls can be observed [30]. HaH 346 chondrite was the last fall officially approved by the Committee of Nomenclature from the HaH DCA. In 1990, in one year, the MetBull database received new records, including the chondrites type: H4, H5, H6 (in a total of 22 specimens from the H group), L5, L6 (in a total of 14 specimens from the L group), and LL6 (one specimen). Several independent falls can occur each year in a DCA region [30]. The problem with the identification of ordinary chondrites is pretty large. This fact generates misunderstandings and nomenclature errors. Therefore, the approved meteorites should be controlled, and their origin should be confirmed. Various spectrometric methods and chemometric approaches can be used as tools in a scientific investigation.

1. A unique low-background gamma-ray spectrometric system was applied to obtain high measurement precision with a low counting rate in chondrite samples. The activities of the radioactive isotopes ^{54}Mn , ^{26}Al , ^{40}K , ^{22}Na , and ^{60}Co in the chondrites collected during two different expeditions were analyzed and compared.
2. Several statistical approaches, including K-means, PCA, and cluster analysis, have been applied to confirm the origins of all specimens from two different campaigns. A chemometric analysis based on a multivariate analysis of short-lived nuclides concentrations confirmed the lack of an affinity of two from a total of ten investigated ordinary chondrites. A chemometric analysis with many variables of short-lived radionuclides is more appropriate for handling a scientific investigation, but statistical (significant) differences do not explain the reason for such a difference between specimens; therefore, other more detailed analysis should be applied for the confirmation of the reason of difference.
3. The dissimilar chondrites are: HaH 346-163 and HaH 346-198, which seem to be statistically different than the other eight chondrites (HAH 346-3, HAH 346-6, HAH 346-7, HaH 346-134, HaH 346-200, HaH 346-201, HaH 346-207, and HaH 346-120, all classified as ordinary chondrite L5). The difference in radionuclide concentrations could be the result of various physical or chemical parameters, especially fluctuating with the pre-atmospheric size of the object (various nuclear channel efficiencies, changes in the energy of particles interacting with the object, inhomogeneity of the structure) and volatility of various elements (boiling point K > Na > Mn > Al > Co).
4. Short-lived radionuclides are sensitive tools to estimate the terrestrial age of chondrites, even if the fall took place in a relatively short time interval. With a short half-life of 312 days, ^{54}Mn is the most representative for a comparison of specimens originating from different falls. Radioactivity levels of ^{54}Mn in HaH 346-163 and HaH 346-198, is on average, twice lower than in the case of other specimens and are equal to 13.3 and 22.5 Bq/kg, while the average value for other specimens is equal to 35.9 ± 7.2 Bq/kg. The short-lived radioactivity levels in the HaH 346 chondrites are consistent with a recent fall (the observed fireball of November 2017).

Author Contributions: M.D.-L. lead project conceptualization, planned and conducted its realization, collected data, analyzed data, and wrote the manuscript; M.K. prepared macroscopic and microscopic photos; M.K., T.J. and A.E. edited and corrected the text of the manuscript and borrowed chondrites to analyse. All authors have read and agreed to the published version of the manuscript.

Funding: This research received no external funding.

Data Availability Statement: The data that support the findings of this study are available from the authors upon request.

Acknowledgments: The author thanks anonymous reviewers for their valuable comments which improved the quality of this manuscript and the Libyan Society for Meteorites and Space Observation for the loan of specimens for analysis.

Conflicts of Interest: The authors declare that they have no conflict of interest.

References

1. Schlüter, J.; Schultz, L.K.; Thiedig, F.; Al-Mahdi, B.O.; Aghreb, A.E. The Dar al Gani meteorite field (Libyan Sahara): Geological setting, pairing of meteorites, and recovery density. *Meteorit. Planet. Sci.* **2002**, *37*, 1079–1093. [[CrossRef](#)]
2. Reedy, R.C.; Arnold, J.R.; Lal, D. Cosmic-ray record in solar system matter. *Annu. Rev. Nucl. Part. Sci.* **1983**, *33*, 505–537. Available online: www.annualreviews.org (accessed on 18 November 2021). [[CrossRef](#)]
3. Leya, I.; Masarik, J. Cosmogenic nuclides in stony meteorites revisited. *Meteorit. Planet. Sci.* **2009**, *44*, 1061–1086. [[CrossRef](#)]
4. Povinec, P.P.; Sýkora, I.; Macke, R.J.; Tóth, J.; Kornoš, L.; Porubčan, V. Radionuclides in Chassigny and Nakhla meteorites of Mars origin: Implications for their pre-atmospheric sizes and cosmic-ray exposure ages. *Planet. Space Sci.* **2020**, *186*, 104914. [[CrossRef](#)]
5. Alexeev, V.A.; Laubenstein, M.; Povinec, P.P.; Ustinova, G.K. Variations of cosmogenic radionuclide production rates along the meteorite orbits. *Adv. Space Res.* **2015**, *56*, 766–771. [[CrossRef](#)]
6. Gladysheva, O.G. Disintegration of the Chelyabinsk cosmic body. *Planet. Space Sci.* **2019**, *178*, 104709. [[CrossRef](#)]

7. Taricco, C.; Bhandari, N.; Colombetti, P.; Verma, N.; Vivaldo, G. Experimental set-up and optimization of a gamma-ray spectrometer for measurement of cosmogenic radionuclides in meteorites. *Nucl. Instrum. Methods Phys. Res. Sect. A Accel. Spectrom. Detect. Assoc. Equip.* **2007**, *572*, 241–243. [[CrossRef](#)]
8. Guan, Y.; Huss, G.R.; Leshin, L.A. SIMS analyses of Mg, Cr, and Ni isotopes in primitive meteorites and short-lived radionuclides in the early solar system. *Appl. Surf. Sci.* **2004**, *231*–*232*, 899–902. [[CrossRef](#)]
9. Hsu, W. Short-lived radionuclides in the early solar system—A meteoritic perspective of the solar system formation. *Chin. Astron. Astrophys.* **2003**, *27*, 365–373. [[CrossRef](#)]
10. Johnston, P.N.; Hulta, M.; Altitzoglou, T. Measurement of low levels of ^{26}Al from meteorite samples. *Appl. Radiat. Isot.* **2002**, *56*, 399–403. [[CrossRef](#)]
11. Arnold, D.; Neumaiera, S.; Sima, O. Deep underground gamma spectrometric measurement of ^{26}Al in meteorite samples. *Appl. Radiat. Isot.* **2002**, *56*, 405–408. [[CrossRef](#)] [[PubMed](#)]
12. Anderson, S.; Benedi, G.K.; Forman, L.V.; Daly, L.; Greenwood, R.C.; Franchi, I.A.; Friedrich, J.M.; Macke, R.; Wiggins, S.; Britt, D.; et al. Mineralogy, petrology, geochemistry, and chronology of the Murrili (H5) meteorite fall: The third recovered fall from the Desert Fireball Network. *Meteorit. Planet. Sci.* **2021**, *56*, 241–259. [[CrossRef](#)]
13. Eugster, O.; Beer, J.; Burger, M.; Finkel, R.C.; Hofmann, H.J.; Krähenbühl, U.; Michel Th Synal, H.A.; Wölfli, W. History of the paired lunar meteorites MAC88104 and MAC88105 derived from noble gas isotopes, radionuclides, and some chemical abundances. *Geochim. Cosmochim. Acta* **1991**, *55*, 3139–3148. [[CrossRef](#)]
14. Evans, J.C.; Reeves, J.H.; Rancitelli, L.A.; Bogard, D.D. Cosmogenic nuclides in recently fallen meteorites: Evidence for galactic cosmic ray variations during the period 1967–1978. *J. Geophys. Res.* **1982**, *87*, 5577–5591. [[CrossRef](#)]
15. Bischoff, A.; Barrat, J.A.; Berndt, J.; Borovicka, J.; Burkhardt, C.; Busemann, H.; Hakenmüller, J.; Heinlein, D.; Hertzog, J.; Kaiser, J.; et al. The Renchen L5-6 chondrite breccia—The first confirmed meteorite fall from Baden-Württemberg (Germany). *Geochemistry* **2019**, *79*, 125525. [[CrossRef](#)]
16. Ogurtssov, M.G. Cosmogenic ^{44}Ti in meteorites—A divergence with ^{14}C and ^{10}Be data. *Adv. Space Res.* **2021**, *68*, 1519–1524. [[CrossRef](#)]
17. Dilg, W.; Mannhart, W.; Steichele, E.; Arnold, P. Precision Neutron Total Cross Section Measurements On Gold And Cobalt In The 40micro-Ev To 5 Milli-EVZeitschrift fuer. *Physik* **1973**, *264*, 427. [[CrossRef](#)]
18. Laubenstein, M.; Giampaoli, A.; Janowski, P.; Mietelski, J.W. Cosmogenic Radionuclides In The Soltmany L6 Meteorite. *Meteorites* **2012**, *2*, 45–51. [[CrossRef](#)]
19. Beno, J.; Breier, R.; Masarik, J. Effects of solar activity on production rates of short-lived cosmogenic radionuclides. *Meteorit. Planet. Sci.* **2020**, *55*, 1048–1056. [[CrossRef](#)]
20. Welten, K.C.; Caffee, M.W.; Hillegonds, D.J.; Masarik, J.; Nishiizumi, K. Identifying large chondrites using cosmogenic radionuclides. *Nucl. Instrum. Methods Phys. Res. Sect. B Beam Interact. Mater. At.* **2010**, *268*, 1185–1188. [[CrossRef](#)]
21. Mahajan, R.R. Noble gases, cosmic ray exposure and radiogenic ages in selected ordinary chondrites. *Adv. Space Res.* **2022**, *70*, 2112–2132. [[CrossRef](#)]
22. Peplowski, P.N.; Wilson, J.T.; Burks, M.; Beck, A.W.; Jun, I.; Lawrence, D.J.; Yokley, Z.W. Cosmogenic radionuclide production modeling with Geant4: Experimental benchmarking and application to nuclear spectroscopy of asteroid (16) Psyche. *Nucl. Inst. Methods Phys. Res. B* **2019**, *446*, 43–57. [[CrossRef](#)]
23. Howard, C.; Ferm, M.; Cesaratto, J.; Daigle, S.; Iliadis, C. Radioisotope studies of the Farmville meteorite using $\gamma\gamma$ -coincidence spectrometry. *Appl. Radiat. Isot.* **2014**, *94*, 23–29. [[CrossRef](#)] [[PubMed](#)]
24. Welten, K.C.; Nishiizumi, K.; Finkel, R.C.; Hillegonds, D.J.; Jull, A.J.T.; Franke, L.; Schultz, L. Exposure history and terrestrial ages of ordinary chondrites from The Dar Al Gani Region, Libya. *Meteorit. Planet. Sci.* **2004**, *39*, 481–498. [[CrossRef](#)]
25. Reedy, R.C. Recent advances in studies of meteorites using cosmogenic radionuclides. *Nucl. Instrum. Methods Phys. Res. B* **2004**, *223*–*224*, 587–590. [[CrossRef](#)]
26. Li, S.; Wang, S.; Leya, I.; Li, Y.; Li, X.; Smith, T. Petrology, mineralogy, porosity, and cosmic-ray exposure history of Huaxi ordinary chondrite. *Meteorit. Planet. Sci.* **2017**, *52*, 937–948. [[CrossRef](#)]
27. Herpers, U.; Vogt, S.; Beer, J.; Suter, M.; Wölfli, W. Determination of spallogenic long-lived radionuclides in chondrites by nuclear analytical techniques. *Analyst* **1989**, *114*, 303. [[CrossRef](#)]
28. Girault, F.; Perrier, F.; Moreira, M.; Zanda, B.; Rochette, P.; Teitler, Y. Effective radium-226 concentration in meteorites. *Geochim. Cosmochim. Acta* **2017**, *208*, 198–219. [[CrossRef](#)]
29. Tymiński, Z.; Miśta EKalbarczyk, P. The Oslo meteorite research for cosmogenic radionuclides and the interpretation of the results. *Acta Soc. Metheoritiae Pol.* **2013**, *4*, 115. (In Polish)
30. Jull, A.; Giscard, M.; Hutzler, A.; Schnitzer, C.; Zahn, D.; Burr, G.; Hill, D. Radionuclide Studies of Stony Meteorites from Hot Deserts. *Radiocarbon* **2013**, *55*, 1779–1789. [[CrossRef](#)]
31. Bonino, G.; Cini Castagnoli, G.; Taricco, C.; Bhandari, N.; Killgore, M. Cosmogenic radionuclides in four fragments of the portales valley meteorite shower: Influence of different element Abundances and Shielding. *Adv. Space Res.* **2002**, *29*, 771–782. [[CrossRef](#)]
32. Alexeeva, V.A.; Laubenstein, M.; Povinec, P.P.; Ustinova, G.K. Cosmogenic Radionuclides In Meteorites and Solar Modulation of Galactic Cosmic Rays In the Internal Heliosphere. *Sol. Syst. Res.* **2019**, *53*, 98–115. [[CrossRef](#)]
33. Długosz-Lisiecka, M. Comparison of two spectrometric counting modes for fast analysis of selected radionuclides activity. *J. Radioanal. Nucl. Chem.* **2016**, *309*, 941–945. [[CrossRef](#)]

34. Długosz-Lisiecka, M. Application of modern anticoincidence (AC) system in HPGe γ -spectrometry for the detection limit lowering of the radionuclides in air filters. *J. Environ. Radioact.* **2017**, *169–170*, 104–108. [[CrossRef](#)]
35. Długosz-Lisiecka, M. Chemometric methods for source apportionment of ^{210}Pb , ^{210}Bi and ^{210}Po for 10 years of urban air radioactivity monitoring in Lodz city, Poland. *Chemosphere* **2019**, *220*, 163–168. [[CrossRef](#)]
36. Tillett, A.; Dermigny, J.; Emamian, M.; Tonin, Y.; Bucay, I.; Smith, R.L.; Darken, M.; Dearing, C.; Orbon, M.; Iliadis, C. A low-background $\gamma\gamma$ -coincidence spectrometer for radioisotope studies. *Nucl. Inst Methods Phys. Res.* **2017**, *871*, 66–71. [[CrossRef](#)]
37. Colombetti, P.; Taricco, C.; Bhandari, N.; Sinha, N.; DiMartino, M.; Cora, A.; Vivaldo, G. Low γ activity measurement of meteorites using HPGe–NaI detector system. *Nucl. Instrum. Methods Phys. Res. A* **2013**, *718*, 140–142. [[CrossRef](#)]
38. Konki, J.; Greenlees, P.T.; Jakobsson, U.; Jones, P.; Julin, R.S.; Juutinen, S.; Ketelhut, K.; Hauschild, R.; Kontro, A.-P.; Leppänen, A.; et al. Comparison of gamma-ray coincidence and low-background gamma-ray singles spectrometry. *Appl. Radiat. Isot.* **2012**, *70*, 392–396. [[CrossRef](#)]
39. Sharma, M.K.; Burnett, J.L. Sensitivity and low-energy response of the Small Anode Germanium well detector with ceramic insert. *Nucl. Instrum. Methods Phys. Sect. A Accel. Spectrom. Detect. Assoc. Equip.* **2021**, *988*, 164943. [[CrossRef](#)]
40. Britton, R.; Jackson, M.J.; Davies, A.V. Quantifying radionuclide signatures from a $\gamma\gamma$ coincidence system. *J. Environ. Radioact.* **2015**, *149*, 158–163. [[CrossRef](#)]
41. Suárez-Navarro, J.A.; Moreno-Reyes, A.M.; Gascó, C.; Alonso, M.M.; Puertas, F. Gamma spectrometry and LabSOCS-calculated efficiency in the radiological characterisation of quadrangular and cubic specimens of hardened portland cement paste. *Radiat. Phys. Chem.* **2020**, *171*, 108709. [[CrossRef](#)]
42. Stanić, G.; Nikolov, J.; Tucaković, I.; Mrđa, D.; Todorović, N.; Grahek, Ž.; Coha, I.; Vraničar, A. Angle vs. LabSOCS for HPGe efficiency calibration. *Nucl. Instrum. Methods Phys. Res. Sect. A Accel. Spectrom. Detect. Assoc. Equip.* **2019**, *920*, 81–87. [[CrossRef](#)]
43. Kanellopoulos, C.; Argyraki, A. Multivariate statistical assessment of groundwater in cases with ultramafic rocks and anthropogenic activities influence. *Appl. Geochem.* **2022**, *141*, 105292. [[CrossRef](#)]
44. Rosen, A.V.; Hofmann, B.A.; Von Sivers, M.; Schumann, M. Radionuclide Activities In Recent Chondrite Falls Determined By Gamma-Ray Spectrometry: Implications For Terrestrial Age Estimates. *Meteorit. Planet. Sci.* **2020**, *55*, 149–163. [[CrossRef](#)]